



---

*Research article*

## **Effect of compression molding temperature on the characterization of asbestos-free composite friction materials for railway applications**

**Rahmad Doni Widodo<sup>1,\*</sup>, Rusiyanto<sup>1</sup>, Wahyudi<sup>1</sup>, Melisa Kartika Sari<sup>1</sup>, Deni Fajar Fitriyana<sup>1</sup>, Januar Parlaungan Siregar<sup>2</sup>, Tezara Cionita<sup>3</sup>, Natalino Fonseca Da Silva Guterres<sup>4</sup>, Mateus De Sousa Da Silva<sup>4</sup> and Jamiluddin Jaafar<sup>5</sup>**

<sup>1</sup> Department of Mechanical Engineering, Universitas Negeri Semarang, Semarang 50229, Indonesia

<sup>2</sup> Faculty of Mechanical & Automotive Engineering Technology, Universiti Malaysia Pahang Al-Sultan Abdullah, Pekan 26600, Pahang, Malaysia

<sup>3</sup> Faculty of Engineering and Quantity Surveying, INTI International University, Nilai 71800, Negeri Sembilan, Malaysia

<sup>4</sup> Department of Mechanical Engineering, Dili Institute of Technology, Aimeti Laran Street, Dili-Timor Leste

<sup>5</sup> Faculty of Mechanical and Manufacturing Engineering, Universiti Tun Hussein Onn Malaysia, Parit Raja, Batu Pahat 86400, Johor, Malaysia

\* **Correspondence:** Email: rahmat.doni@mail.unnes.ac.id.

**Abstract:** Brake pads significantly affect the braking performance of railways under both normal and emergency operating conditions. In previous studies, brake pads were made using the hand lay-up method and produced the best properties on specimens with epoxy, rice husk, Al<sub>2</sub>O<sub>3</sub> and Fe<sub>2</sub>O<sub>3</sub> compositions of 50%, 20%, 15% and 15%. However, the resulting density does not meet the density standard set by PT Industri Kereta Api Indonesia (PT INKA), which is 1.7–2.4 g/cm<sup>3</sup>. To date, there has been limited research into the utilization of the compression hot molding method for the production of asbestos-free composite friction materials composed of epoxy, rice husk, Al<sub>2</sub>O<sub>3</sub> and Fe<sub>2</sub>O<sub>3</sub> for railway applications. In this study, we aimed to determine the effect of compression molding temperature on the characterization of composite brake pads for railway applications. The brake pad specimens were made of epoxy resin, rice husk, Al<sub>2</sub>O<sub>3</sub> and Fe<sub>2</sub>O<sub>3</sub> with a composition of 50%, 20%, 15% and 15%, respectively. The manufacture of composites in this study used the compression molding method with a pressure of 20 MPa for 15 min holding time. The mold temperature used were 80, 100, 120 °C. Density, hardness, tensile, wear, thermal gravimetric analysis (TGA) and differential scanning calorimetry (DSC) tests were performed to evaluate

the properties of the specimens obtained. The results demonstrated that an increase in molding temperature improved the characterization of the brake pads, with the best results achieved at a molding temperature of 120 °C (SP-3 specimen). SP-3 specimens had the best density, hardness, tensile properties and thermal properties compared to other specimens.

**Keywords:** brake pads; railways; composites; compression molding; friction materials

---

## 1. Introduction

The effectiveness of brake pads has a significant impact on railways' capacity for stopping in an emergency as well as during normal operations [1]. Brake pads are used as components to ensure the safety of the railways during the braking process. Generally, brake pads on trains can be divided into organic and metal. Organic brake pads, which are composed of organic polymers, have been implemented in cars, trains and other modes of transportation. Metal-based brake pads have emerged as the preferred material for high-speed trains due to their outstanding friction capability, commendable resistance to wear, outstanding thermal conductivity and ability to withstand high operational temperatures [1,2].

Composite brake pads have been used in Indonesia since the last decade to replace cast iron brake pads for trains. Cast iron brake pads wear out faster when compared to composite brake pads [3]. In addition, metallic brake pads have a very high density, which can reduce the energy efficiency of the train system [4]. In recent years, the development of composite technology has made rapid progress with various innovations in the manufacture of brake pads using natural materials that have become waste and are no longer used. Composite itself is a material composed of a mixture of two or more materials with different mechanical properties to produce a new material that has different mechanical properties from its constituent materials. The properties of composite materials are a combination of the properties of its constituents, the matrix and reinforcement or filler. The matrix serves to transfer stress to the fiber, form coherent bonds, protect the fiber and remain stable after the manufacturing process. Reinforcement or filler materials must be able to support or improve the properties of the matrix in fabricating composite materials [5].

In previous studies, brake pads for applications on trains have been successfully made using the hand lay-up method. Brake pads with the best properties were found in specimens with a composition of epoxy, rice husk, Al<sub>2</sub>O<sub>3</sub> and Fe<sub>2</sub>O<sub>3</sub> of 50%, 20%, 15% and 15% respectively and a mesh size of 200. This composition produced density, hardness, tensile strength, specific wear value and degradation temperature of 1.23 g/cm<sup>3</sup>, 81.2 HV, 23.34 MPa,  $8.67 \times 10^{-7}$  N/mm<sup>2</sup> and 379 °C [6]. Moreover, when using 100 mesh rice husk, the density, hardness, specific wear value, and degradation temperature of the resulting composite brake friction material were 1.33 g/cm<sup>3</sup>, 83.4 HV,  $10.8 \times 10^{-7}$  N/mm<sup>2</sup> and 363.99 °C [7]. However, the resulting density does not meet the standard density set by PT. Industri Kereta Api (INKA), which is 1.7–2.4 g/cm<sup>3</sup> [8].

The hand layup method is a commonly employed technique in the fabrication of composite materials. Typically, the initial cost associated with fabricating composites using the hand layup technique is quite economical. Furthermore, this methodology enables the production of items with diverse geometries, structures and designs.

Nevertheless, the hand layup technique employed in composite manufacturing exhibits several limitations, including a reduced production speed and a decreased volume proportion of reinforcement. Furthermore, the use of this technique results in an uneven dispersion of reinforcing and matrix substances as a consequence of the inherent imprecision associated with handling by hand. As a result, producing high-quality composites in large quantities using the hand layup method is not possible [9–11].

Based on the description above, another method is needed to meet the characteristic requirements of brake pads for applications on trains. One method of fabricating composites that can produce better characteristics is compression molding. According to the findings of a study by Nyior et al. (2018), compression molding produced composites with better mechanical properties than the manual lay-up (hand lay-up) method. Their study found that the tensile strength and Young's modulus of samples made with compression molding were 77% and 47% higher than samples made by hand lay-up, respectively. The results also showed that the impact strength of the materials made by compression molding (11.5 kJ/m<sup>2</sup>) was significantly higher than that of the samples made by hand lay-up, which had an impact strength of 7 kJ/m<sup>2</sup> [12].

In general, the components used in brake pads to create friction materials are the matrix or adhesive, reinforcements, fillers and abrasives. The proper combination of these components is critical to ensuring the efficient and reliable functioning of brake pads in various applications, such as brake pads for railways [13]. The high-speed trains usually use special brake block materials consisting of steel wool fiber, resin, aramid fiber, graphite, barium sulfate, magnesium, friction powder, mineral wool fiber, calcium carbonate powder, butyronitrile rubber powder, antimony sulfide and argil [14]. On the other hand, brake pads designed for high-speed and heavy trains are produced using phenolic resin, composite fibers, graphite, barium sulfate, iron powder, butyronitrile, zirconite, rubber powder, feldspar powder and alumina [15]. Moreover, the composite brake block for trains made by Green Power Runde Industry Co. Limited. consists of phenolic resin, nitrile rubber, steel fiber, reduced iron powder, graphite, etc. [16]. In this study, the fabrication of asbestos-free composite friction material specimens for railway applications utilizes a more straightforward combination of materials that include epoxy, rice husk, Al<sub>2</sub>O<sub>3</sub> and Fe<sub>2</sub>O<sub>3</sub>. The roles of epoxy resin, rice husk, Al<sub>2</sub>O<sub>3</sub> and Fe<sub>2</sub>O<sub>3</sub> are as matrix [17], reinforcement [18], filler [19] and abrasive [20,21], respectively. The composite material as friction materials will be pressed and heated at a certain pressure and temperature. Furthermore, the fabrication of asbestos-free composite friction materials for railway applications made from epoxy, rice husk, Al<sub>2</sub>O<sub>3</sub> and Fe<sub>2</sub>O<sub>3</sub> by compression hot molding has not been widely studied. The pressure applied can make the composite tighter and denser. While the heating process makes the resin move to flow to fill the empty composite parts. Our purpose of this study was to determine the effect of compression molding temperature on the characterization of composite brake pads for applications on railways.

## 2. Materials and methods

### 2.1. Materials

The materials used in this study were epoxy, hardener, rice husk, aluminum oxide (Al<sub>2</sub>O<sub>3</sub>) and iron oxide (Fe<sub>2</sub>O<sub>3</sub>). The matrix used in this study was Bisphenol A-Epichlorohydrin epoxy resin as a binder, and Cycloaliphatic Amine type epoxy hardener obtained from the Justus store in Semarang, Indonesia.

In general, epoxy has a density, tensile strength and flexural strength of 1.18 g/cm<sup>3</sup>, 63.7 and 8.3 MPa [22]. The rice husk used in this study was obtained from a rice mill near the campus. The composition of rice husk consists of cellulose (50%), lignin (25%–30%), silica (15%–20%) and the remainder consists of hemicellulose and water content [23]. In this study, Al<sub>2</sub>O<sub>3</sub> and Fe<sub>2</sub>O<sub>3</sub> were obtained from PT Merck Tbk, Indonesia.

## 2.2. Specimen fabrications

In this study, the fabrication of brake pad specimens used the compression molding method. The preparation of raw materials for the fabrication of brake pad specimens refers to previous research [6,7]. The rice husk was crushed using the FOMAC FCT-Z300 miller machine and sieved using a 200 mesh. Furthermore, the specimens were prepared by mixing the materials according to a predetermined concentration using a hand mixer in a plastic cup in stages. First, mixing epoxy and hardener with a ratio of 1:3 was carried out for 7 min. Then, a mixture of rice husk, aluminum oxide, iron oxide was added after being stirred for 5 min. Mixing was done again for 10 min. After all the ingredients were mixed, they were poured into the mold and left to harden at room temperature for up to 10 h. Furthermore, the specimen was compressed with a pressure of 20 MPa for 15 min and a temperature of 80, 100 and 120 °C (Table 1). In this study, the specimen produced at a molding temperature of 80 °C is called specimen number 1 and coded SP-1. The specimen produced at a molding temperature of 100 °C is called specimen number 2 and coded SP-2. While SP-3 is specimen number 3 produced at a molding temperature of 120 °C. After that, the composite specimens were cut and characterized.

**Table 1.** Composite brake pads specimen code and compression molding setting parameters.

Specimen code	Pressure (MPa)	Holding time (min)	Temperature (°C)
SP-1	20	15	80
SP-2	20	15	100
SP-3	20	15	120

## 2.3. Testing and characterizations

In this study, the tests carried out were density, hardness, tensile and wear using the Ogoshi method, thermal gravimetric analysis (TGA) and differential scanning calorimetry (DSC). Density testing was based on ASTM D792 standard. Density testing was performed using an electronic density meter DME 220 series from Vibra Canada Inc. (Mississauga, ON, USA). This test is carried out by weighing the dry mass and the mass of the test object in water (wet mass). Vickers hardness testing in this study refers to the testing method carried out by [6,24]. Hardness testing was carried out using a Microhardness Tester F-800 machine (Future-Tech Corp., Kanagawa, Japan) with a test load of 25 gf and a dwell time of 10 s. Tensile testing was done according to the ASTM D638 standard using a HT-2402 Computer Servo Control Material Testing Machines from Hung Ta Instrument Co., Ltd., Samutprakarn, Thailand. The tensile test results consist of max force and elongation, which will be used to calculate the tensile strength and tensile modulus. Wear testing was performed using the Oghosi High Speed Universal Wear Testing Machine (Type OAT-U). The Ogoshi wear test was carried out

with the width of the wear plate ( $B$ ) = 3 mm, the radius of the wear plate ( $r$ ) = 13.06 mm, the distance traveled during the wear process ( $l$ ) = 66.6 m and the test load ( $F$ ) = 2.12 kg. The TGA test was carried out based on the ASTM D6370 standard using the NEXTA STA test kit (Hitachi STA200RV with Real View Sample Observation). The temperature used in this test was 30–550 °C. The testing process was conducted at a heating rate of 10 °C/min with a 100 mL/min nitrogen gas flow.

The test results obtain the temperature and weight loss values. The DSC test was carried out based on the ASTM D3418 standard using the NEXTA STA test tool (Hitachi STA200RV with Real View Sample Observation). The temperature used in this test was 30–550 °C. The testing process was carried out at a heating rate of 10 °C/min with a nitrogen gas flow of 100 mL/min. The test results obtain the temperature and heat flow values of the composite specimens.

### 3. Results and discussion

#### 3.1. Effect of compression molding temperature on the density of brake pad composite specimens

Figure 1 shows the density of composite brake pad specimens with variations in molding temperature. The results of this study indicated that the increase in temperature affected the results of the composite density. The lowest density was shown in the SP-1 specimen, which was 1.695 g/cm<sup>3</sup>. While the highest density was shown in the SP-3 specimen, which was 1.701 g/cm<sup>3</sup>. The increase in density value occurs due to an increase in the temperature of composite fabrications with the compression molding method which causes a decrease in the viscosity of the resin, making it easier for the polymer to fill voids [25,26]. The fewer voids produced, the greater the density of the brake pad samples [6]. Void content is the percentage by volume of empty spaces or cavities inside composite materials [26]. When there are voids in a composite, they occupy space that would otherwise be occupied by the composite material. As a consequence, the composite's overall density decreases as the total mass is distributed over a larger volume [6,26].

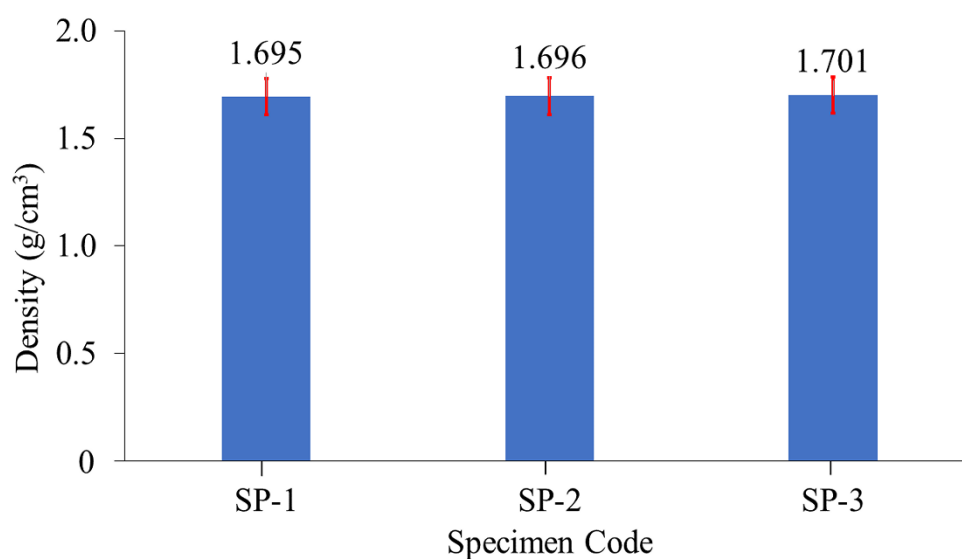


**Figure 1.** Effect of compression molding temperature on the density of brake pad composite specimens.

In the manufacture of brake pad specimens using the compression molding method, an increase in molding temperature causes the viscosity of the resin to decrease so that the resin flows more easily and wets the reinforcing material. This results in a better bond between the resin, filler and reinforcement, resulting in an increase in the density of the composite specimen [6]. This is what causes SP-3 to have a higher density than other composite specimens. Incomplete resin flow into the desiccated area of reinforcement and filler materials can give rise to porosity in composite specimens. This is typically the result of increased resin viscosity due to exposure to ambient conditions and low-temperature curing cycles, resulting in inadequate flow. The lowered molding temperature reduces the driving force of gas-induced cavity growth, so that more porosity is produced, resulting in a decrease in the specimen's mechanical properties [26–29].

The results of this investigation are consistent with Ochi et al.'s (2015) research. Their findings demonstrated a correlation between the density of long bamboo fiber/PLA Composites and the temperature of the mold. In general, the density of composites increases from 140 to 160 °C as the molding temperature. However, when the molding temperature exceeds 160 °C, the density of the composite decreases. This occurs because mold temperatures above 160 °C reduce the matrix's viscosity and make it simpler for air to become trapped inside the material during the molding process, resulting in the formation of numerous voids [30]. In another study, Ochi et al. (2022) demonstrated the relationship between the density of bamboo fiber bundle-reinforced bamboo powder composite materials and the molding temperature. As the molding temperature increased, the density of the composite specimens remained relatively constant. The density of composites was between 1.41 and 1.42 g/cm<sup>3</sup> [31].

Based on these research results, only the SP-3 specimen met the minimum density determined by PT INKA, which was 1.7–2.4 g/cm<sup>3</sup> [8]. Furthermore, the density of the SP-2 and SP-1 specimens almost met the specified density requirements. In addition, the density obtained in this study was higher than the results of previous studies. In previous research, brake pad composite fabrication used the hand layup method with various compositions. The highest densities produced in previous studies were 1.23 [6] and 1.33 g/cm<sup>3</sup> [7]; whereas in this study, the densities of the specimens SP-1, SP-2 and SP-3 were 1.695, 1.696 and 1.701 g/cm<sup>3</sup>, respectively.

### *3.2. Effect of compression molding temperature on the hardness of brake pad composite specimens*

The effect of temperature on the hardness of the composite is shown in Figure 2. The lowest hardness value was shown in the SP-1 specimen, which was 96.9 gf/mm<sup>2</sup> (HV), while the highest density was shown in the SP-3 specimen, which was 108.2 gf/mm<sup>2</sup> (HV). SP-3 and SP-1 specimens were the specimens with the highest and lowest densities produced in the study, respectively. In general, the hardness of composite specimens increases in proportion to their density. This is due to the fact that dense materials have strong interfacial bonding's between their matrix and reinforcement, making them more resistant to indentation and plastic deformation [6,32].

Previous research reached the same conclusion, which is that the specimen's higher density increased its hardness [33–36]. Research conducted by Fouly et al. (2021) showed that increasing the density of the composite causes an increase in the hardness of the specimen. Therefore, the average hardness also increases with increasing density. The poly(methyl methacrylate) (PMMA) nanocomposites specimen reinforced with 8 wt.% hydroxyapatite (PMHA8) specimen obtained a maximum hardness of 87.7 D-index. This happened because the PMHA8 specimen had the highest density compared to

the other specimens [32]. Furthermore, an increase in the composite is hardness indicates a good interfacial bond between the matrix and the reinforcing fiber. The stronger the interfacial bond between the matrix and the reinforcing fiber, the higher the hardness of the resulting composite specimen [37,38]. Yawas et al. obtained the maximum hardness and density of non-asbestos brake pad samples using a compaction load and sintering temperature of 15 t and 150 °C, respectively. This happens because using these variations results in a more uniform distribution of frictional filler material particles in the matrix. Furthermore, this variation increases the surface area, which improves the matrix's bonding ability with frictional filler material [39].

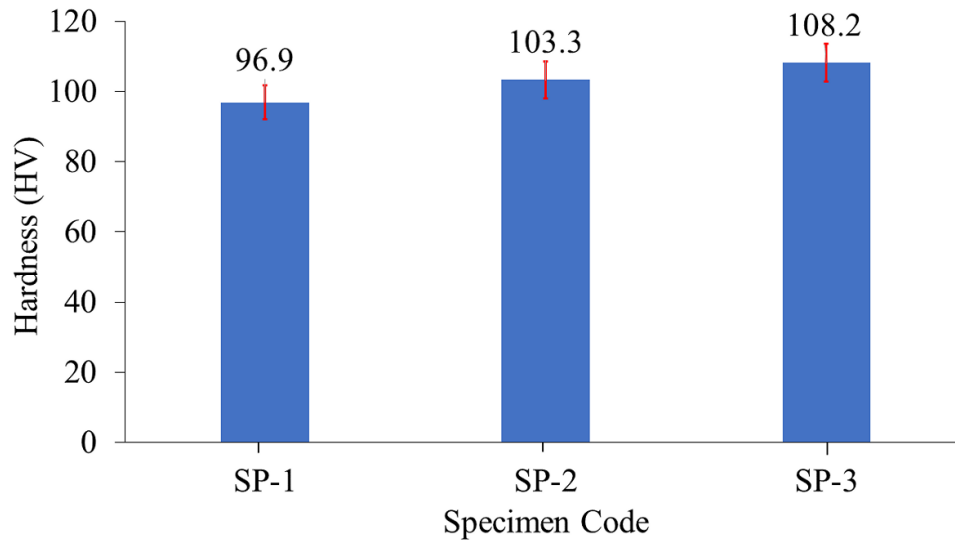


**Figure 2.** Effect of compression molding temperature on the hardness of brake pad composite specimens.

### 3.3. Effect of compression molding temperature on the tensile strength of brake pad composite specimens

The effect of temperature on the tensile strength of the composite is shown in Figure 3. The lowest tensile strength value was shown in the SP-1 specimen, which was 7.26 MPa, while the highest tensile strength was shown in the SP-3 specimen, which was 26.22 MPa.

The increase in the value of tensile strength is affected by the behavior of the bond between the resin and fiber interfaces at each increasing compression molding temperature variation [40]. This is in line with research conducted by Sumesh et al. (2020). Composites with an epoxy resin matrix formed by the compression molding method produce the best mechanical properties of tensile strength at higher temperatures [41].

Heating at high temperatures facilitates the mobilization of the resin in fiber impregnation. The increase in tensile strength is also due to an increase in mold temperature, which reduces the viscosity of the matrix which has an impact on reducing voids in the composite [42].

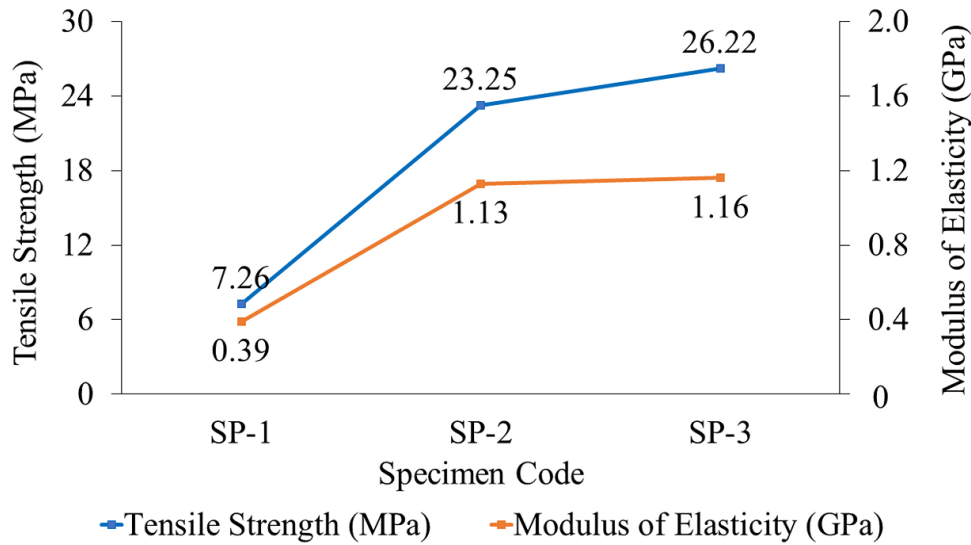


**Figure 3.** Effect of temperature on tensile strength and tensile modulus of brake pad composite specimens.

The increase in tensile strength may also be caused by the main process that occurs at a molding temperature of 80–120 °C for the evaporation. The higher the molding temperature, the higher the moisture content in the evaporating fiber, therefore the higher the tensile strength. Mvondo et al. (2017) stated that there was a negative relationship between the moisture content of tropical wood fiber and its tensile strength. Differences in the percentage of water content in fiber were studied. In fibers that have a lower water content produces high tensile strength, while high water content produces low tensile strength [43]. Figure 3 shows that the modulus of elasticity had increased with increasing molding temperature. The modulus of elasticity represents the inflexibility of a material [44,45]. The higher the value of the modulus of elasticity is, the less flexible the material. At higher molding temperatures, the specimen becomes stiffer so that the modulus value is higher [18,19]. In accordance with research conducted by Ochi et al. (2022) [31], the value of the elastic modulus increased with increasing temperature used in the specimen molding process using the compression molding method.

#### 3.4. Effect of compression molding temperature on the specific wear of brake pad composite specimens

The wear test results showed that the use of higher mold temperatures can cause a decrease in the wear resistance of the composite (Figure 4). A higher specific wear value indicated a lower wear resistance property. In the study, the SP-3 specimen had the highest specific wear value of  $15.08 \times 10^{-7} \text{ mm}^2/\text{kg}$  while the SP-2 specimen had the lowest specific wear value. Thus, it can be said that the highest wear resistance was found in the SP-2 specimen. According Günay et al. (2020), a negative correlation exists between a material's hardness value and the specific wear value it exhibits. Materials possessing high hardness exhibit enhanced resistance to wear and tear, hence endowing the test specimens with excellent wear resistance.



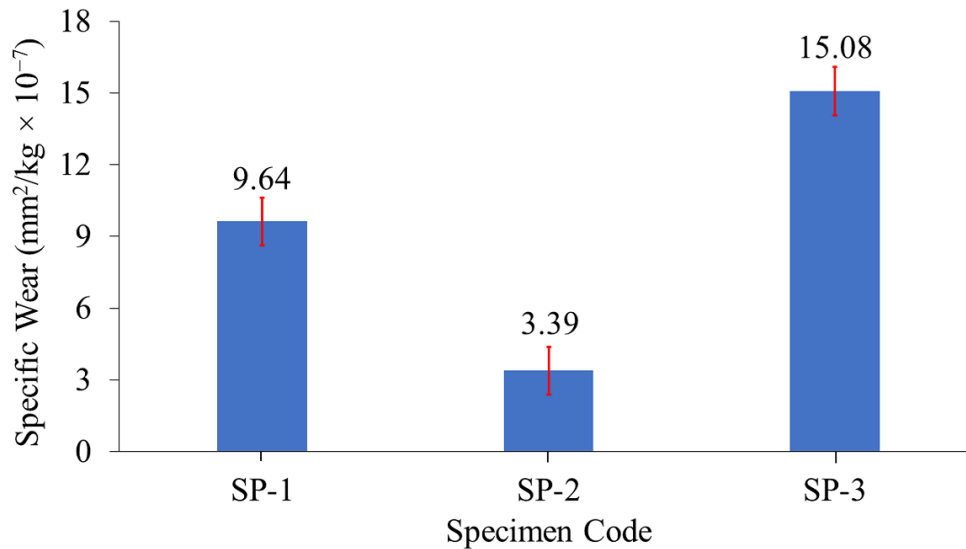


**Figure 4.** Effect of compression molding temperature on the specific wear of brake pad composite specimens.

The reason for this phenomenon is that the wear value acquired during Ogoshi wear testing exhibits an inverse relationship with the wear resistance qualities of the material being tested. A material's wear resistance qualities are improved when its specific wear value decreases [46].

Nevertheless, this investigation revealed that SP-3 had the highest specific wear value. It can be asserted that SP-3 exhibits the lowest level of wear resistance. This phenomenon can be attributed to the positive correlation between the temperature applied and the surface roughness observed in the composite specimen. The findings of a study conducted by Jan et al. (2020) indicate that elevating the temperature of the mold leads to a corresponding increase in the roughness of the composite material. Their findings indicated that elevating the mold temperature led to a corresponding increase in the surface roughness of the brake pad [47]. The occurrence of increased surface roughness in the specimen can be attributed to the roughness of the composite surface when it comes into contact with the surface of the hard steel disc (used as test equipment). This contact leads to the formation of cracks on both the surface and subsurface of the specimen, which results in matrix delamination or wear [48]. This results in the removal of material in large flakes and creates various irregular edge shapes resulting in higher friction and wear [48].

### 3.5. Effect of compression molding temperature on the thermal properties of brake pad composite specimens

TGA and DSC testing in this study was conducted to determine the thermal properties of the composite. Figure 5 shows that the composite brake pads specimen had several temperature variations during thermal decomposition that occurred in the temperature range of 30–550 °C. Weight loss on initial heating (30–200 °C) was caused by the evaporation of water on the rice husk. This happened because water was not chemically bound to the fiber. The reduction of fiber mass was further related to the degradation of hemicellulose. In the second range (200–400 °C), the weight loss that occurred was mostly due to the decomposition of hemicellulose and cellulose fibers and was followed by the

decomposition of epoxy resin. In the last range (400–550 °C), the weight loss that occurred was caused by fiber degradation and decomposition of epoxy resin and filler.

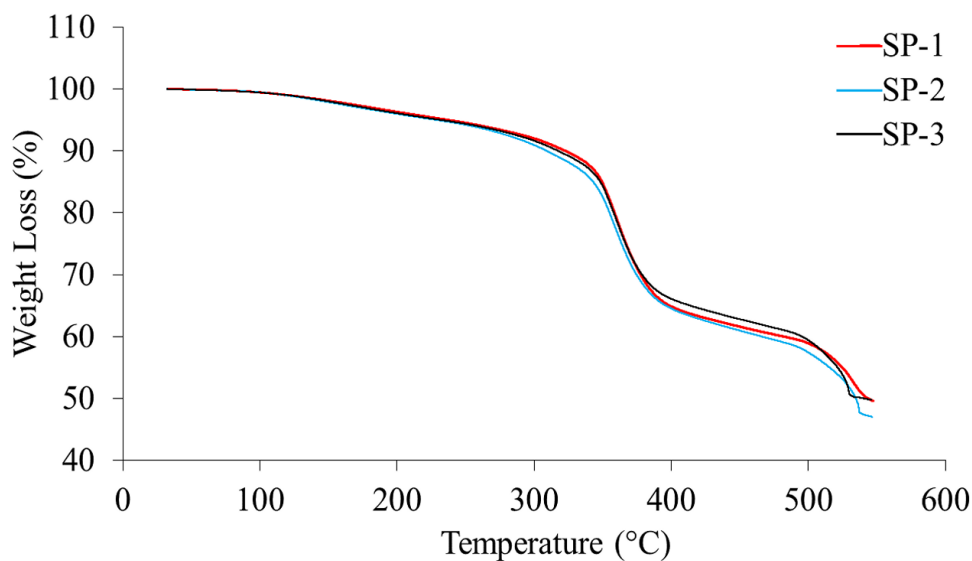


**Figure 5.** Effect of compression molding temperature on composite weight loss.

This is in accordance with research conducted by Chen et al. (2020), rice husk experiences weight loss which is divided into three stages. At a temperature of 35–150 °C, rice husk undergoes evaporation of water in the fiber. At temperatures of 150–380 °C decomposition of hemicellulose, cellulose and lignin occurs and at temperature stages of 380–600 °C fiber degradation occurs [49]. The TGA test with a temperature scale of 30–550 °C resulted in a residue of 49.48% in the SP-1 specimen, 46.97% in the SP-2 specimen and 49.94% in the SP-3 specimen. The residual results in this study are in line with research by Li et al. (2020), the residual weight of the composite showed a tendency to increase with increasing molding temperature. The results of the TGA curve analysis show that the right molding temperature will help the curing reaction and cross-linking of resin and fiber. The increased crosslink density of the composite will strengthen the thermal stability of the composite [50].

Figure 6 shows the derivative thermal gravimetry (DTG) curve for each composite brake pads specimen that experienced a maximum decomposition phase ( $T_{max}$ ) concerning temperature, which was shown at the main peak. SP-1 specimen occurred at 359.98 °C, SP-2 specimen at 356.13 °C and SP-3 specimen at 360.94 °C. Maximum decomposition is the maximum weight loss on the specimen that occurs at a certain temperature ( $T_{max}$ ), which can be used as the most important indicator in determining the thermal stability of a material [51]. The results showed that there was an effect of the use of specimen molding temperature. The specimen with a molding temperature of 120 °C had a larger  $T_{max}$  and residue than other specimens. According to research by Li et al. (2020), by increasing the molding temperature, the durability of the epoxy resin and fiber activity tends to increase, which benefits the chemical bond between the fiber and the resin which results in increased composite cross-linking so that the degradation temperature will be higher [50].

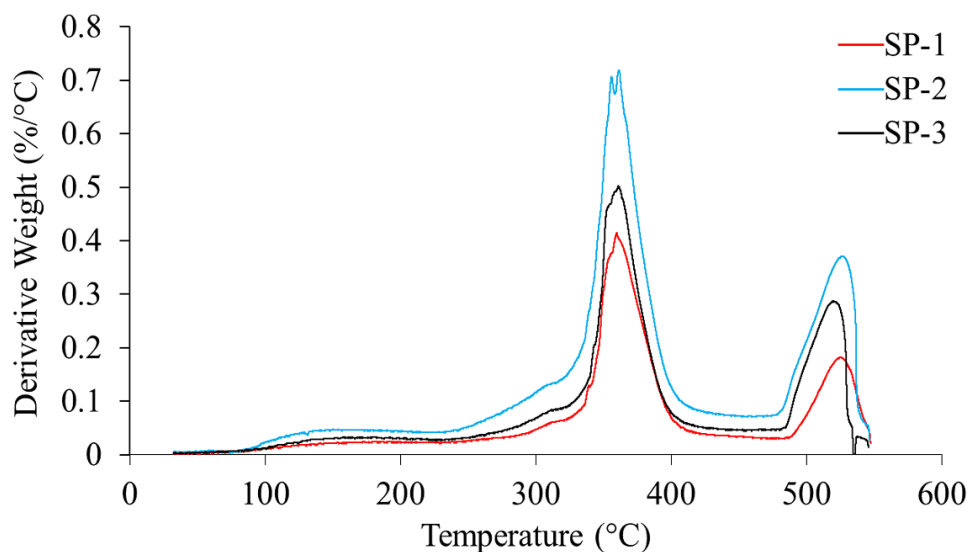


**Figure 6.** The effect of compression molding temperature on the derivative weight of the composite.

Based on Figure 7, the exothermic phase occurred when heated to a temperature of 30–550 °C. On the DSC curve, glass transition temperature ( $T_g$ ) can be known from each specimen. The glass temperature is the transition temperature where the behavior of the composite transitions from hard glass to soft rubber [52]. The SP-1 specimen had a  $T_g$  of 311.25 °C. The SP-2 specimen had a  $T_g$  of 309.18 °C. The SP-3 specimen had a  $T_g$  of 310.06 °C. After passing through the  $T_g$  material, each specimen began to form crystals. Specimens will experience cold crystallization; cold crystallization is a unique phenomenon in which crystallization that accompanies an exothermic anomaly occurs when a material is heated to a temperature below its melting point but above the temperature of its glass. On the curve, the peak point of the curve after going through the  $T_g$  phase is crystallization temperature ( $T_c$ ). Temperature crystallization is a transition temperature where the formation of a crystal structure occurs due to heating [53].

The SP-1 specimen has the highest  $T_c$  of 526.17 °C. The SP-2 specimen has the highest  $T_c$  of 529.83 °C. The SP-3 specimen has the highest  $T_c$  of 523.17 °C. The three specimens did not experience an endothermic phase, in which the specimens did not melt up to 550 °C. On the DSC curve, temperature melting ( $T_m$ ) can be observed at the turning point of the curve. This is in line with Li et al. (2020), which stated that the first exothermic peak is closely related to the glass transition. Increased  $T_g$  and decreased peaks can be attributed to increased crosslinking and amorphism. The decreasing exothermic peak value of the composite indicates that the crosslink density of the mixture is increasing. It can be concluded that a reasonable increase in molding temperature will be conducive to increasing the crosslink density [50].

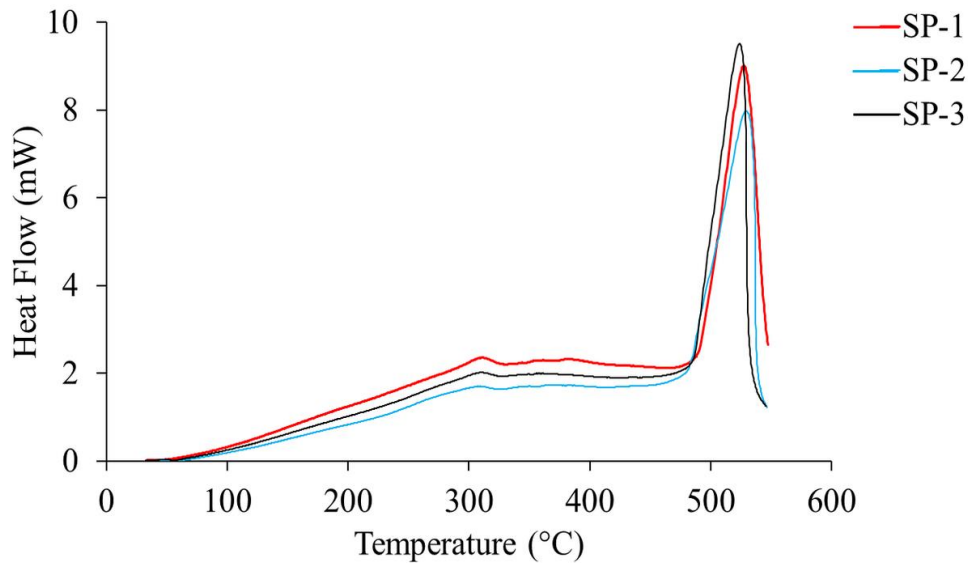


**Figure 7.** Effect of compression molding temperature on composite heat flow.

#### 4. Conclusions

The effect of compression molding temperature on the characterization of asbestos-free composite friction materials for railway applications has been discussed in this study. Density, hardness, tensile, wear, TGA and DSC tests were performed to evaluate the properties of the obtained specimens. According to our findings, increasing the temperature during the compression molding process reduces the viscosity of the resin, allowing the resin to flow more easily and wet the reinforcement, filler and abrasive materials. This leads to better bonding between the constituent materials, so the density of the composite specimen increases. The mechanical and thermal properties of the composite specimens increase as density increases. The results of this study show that specimen SP-3 has better characteristics compared to other specimens. The density, Vickers hardness, tensile strength and tensile modulus of SP-3 specimens are 1.70 g/cm<sup>3</sup>, 108.2 HV, 26.25 MPa and 1.16 GPa, respectively. The highest thermal properties were generated by SP-3 specimen, with total residues, T<sub>max</sub>, T<sub>g</sub> and T<sub>c</sub> values of 49.94%, 360.94, 310.06 and 517.17 °C, respectively. Furthermore, the molding temperature has a significant effect on the specific wear on the composite specimen. Specific wear ( $\times 10^{-7}$  mm<sup>2</sup>/kg) on SP-1, SP-2 and SP-3 specimens were 9.64, 3.49 and 15.08, respectively.

#### Use of AI tools declaration

The authors declare that they have not used Artificial Intelligence (AI) tools in the creation of this article.

#### Acknowledgments

The authors would like to express their gratitude to the Faculty of Engineering, Universitas Negeri Semarang, for giving funding through the Penelitian Kerja Sama Antar Lembaga (FAKULTAS) Grant No.: 11.17.4/UN37/PPK.05/2023.

## Conflict of interest

The authors declare no conflicts of interest.

## References

1. Xiao JK, Xiao SX, Chen J, et al. (2020) Wear mechanism of Cu-based brake pad for high-speed train braking at speed of 380 km/h. *Tribol Int* 150: 106357. <https://doi.org/10.1016/j.triboint.2020.106357>
2. Zhang P, Zhang L, Wei D, et al. (2020) A high-performance copper-based brake pad for high-speed railway trains and its surface substance evolution and wear mechanism at high temperature. *Wear* 444–445: 203182. <https://doi.org/10.1016/j.wear.2019.203182>
3. Mazur VL, Naidek VL, Popov YS (2021) Comparison of cast-iron and composite brake pads with cast-iron inserts for rolling stock of railways. *Met Cast Ukr* 29: 30–39. <http://dx.doi.org/10.15407/steelcast2021.02.080>
4. Ammar Z, Ibrahim H, Adly M, et al. (2023) Influence of natural fiber content on the frictional material of brake pads: A review. *J Compos Sci* 7: 72. <https://doi.org/10.3390/jcs7020072>
5. Nuryanta MI, Aryaswara LG, Korsmik R, et al. (2023) The interconnection of carbon active addition on mechanical properties of hybrid agel/glass fiber-reinforced green composite. *Polymers* 15: 2411. <https://doi.org/10.3390/polym15112411>
6. Irawan AP, Fitriyana DF, Siregar JP, et al. (2023) Influence of varying concentrations of epoxy, rice husk, Al<sub>2</sub>O<sub>3</sub>, and Fe<sub>2</sub>O<sub>3</sub> on the properties of brake friction materials prepared using hand layup method. *Polymers* 15: 2597. <https://doi.org/10.3390/polym15122597>
7. Khafidh M, Putera FP, Yotenka R, et al. (2023) A study on characteristics of brake pad composite materials by varying the composition of epoxy, rice husk, Al<sub>2</sub>O<sub>3</sub>, and Fe<sub>2</sub>O<sub>3</sub>. *Automot Exp* 6: 303–319. <https://doi.org/10.31603/ae.9121>
8. PT Inka Multi Solusi Trading (2019) Brake shoe composite. Available from: <https://imst.id/id/products/brake-shoe-composite-3/> (accessed on 6 December 2023).
9. Maiti S, Islam MR, Uddin MA, et al. (2022) Sustainable fiber-reinforced composites: A review. *Adv Sustainable Syst* 6: 2200258. <https://doi.org/10.1002/adsu.202200258>
10. Nugraha AD, Nuryanta MI, Sean L, et al. (2022) Recent progress on natural fibers mixed with CFRP and GFRP: Properties, characteristics, and failure behaviour. *Polymers* 14: 5138. <https://doi.org/10.3390/polym14235138>
11. Sałasińska K, Cabulis P, Kirpluks M, et al. (2022) The effect of manufacture process on mechanical properties and burning behavior of epoxy-based hybrid composites. *Materials* 15: 301. <https://doi.org/10.3390/ma15010301>
12. Nyior GB, Mgbeahuru EC (2018) Effects of processing methods on mechanical properties of alkali treated bagasse fibre reinforced epoxy composite. *J Miner Mater Charact Eng* 6: 345–355. <https://doi.org/10.4236/jmmce.2018.63024>
13. Irawan AP, Fitriyana DF, Tezara C, et al. (2022) Overview of the important factors influencing the performance of eco-friendly brake pads. *Polymers* 14: 1180. <https://doi.org/10.3390/polym14061180>
14. Du DS, Tian SG, Yan J, et al. (2008) Composite material brake block special for high-speed train. China Patent No. CN101435475A.

15. Lv HC (2000) Composite brake shoe with great friction coefficient and its manufacture. China Patent No. CN1344640A.
16. Shi C (2023) Composite brake block for railway. Available from: <https://green-power123.en.made-in-china.com/product/1XHnGBmAsOkx/China-Composite-Brake-Block-for-Railway.html> (accessed on 29 November 2023).
17. Abutu J, Lawal SA, Ndaliman MB, et al. (2018) Effects of process parameters on the properties of brake pad developed from seashell as reinforcement material using grey relational analysis. *Eng Sci Technol* 21: 787–797. <https://doi.org/10.1016/j.jestch.2018.05.014>
18. Nandiyanto ABD, Hofifah SN, Girsang GCS, et al. (2021) The effects of rice husk particles size as a reinforcement component on resin-based brake pad performance: From literature review on the use of agricultural waste as a reinforcement material, chemical polymerization reaction of epoxy resin, to experiments. *Automot Exp* 4: 68–82. <https://doi.org/10.31603/ae.4815>
19. Pinca-Bretotean C, Josan A, Sharma AK (2023) Composites based on sustainable biomass fiber for automotive brake pads. *Mater Plast* 60: 33–41. <https://doi.org/10.37358/Mat.Plast.1964>
20. Majeed B, Basturk S (2020) Analysis of polymeric composite materials for frictional wear resistance purposes. *Polym Polym Compos* 29: 127–137. <https://doi.org/10.1177/0967391120903957>
21. Olaitan AJ, Chidome AJ (2020) Development of polymer-matrix composite material using banana stem fibre and bagasse particles for production of automobile brake pad. *Int J Mech Eng* 5: 46–55.
22. Primaningtyas WE, Sakura RR, Suheni S, et al. (2019) Asbestos-free brake pad using composite polymer strengthened with rice husk powder. *IOP Conf Ser Mater Sci Eng* 462: 012015. <https://doi.org/10.1088/1757-899X/462/1/012015>
23. Fuadi AM, Ataka F (2020) Pembuatan Kertas dari Limbah Jerami dan Sekam Padi dengan Metode Organosolv. *Simp Nas RAPI* 19: 33–38. Available from: <https://publikasiilmiah.ums.ac.id/bitstream/handle/11617/12375/105.pdf?sequence=1&isAllowed=y>.
24. Sharma A, Choudhary M, Agarwal P, et al. (2021) Effect of micro-sized marble dust on mechanical and thermo-mechanical properties of needle-punched nonwoven jute fiber reinforced polymer composites. *Polym Composite* 42: 881–898. <https://doi.org/10.1002/pc.25873>
25. Fazli A, Stevanovic T, Rodrigue D (2022) Recycled HDPE/natural fiber composites modified with waste tire rubber: A comparison between injection and compression molding. *Polymers* 14: 3197. <https://doi.org/10.3390/polym14153197>
26. Mehdikhani M, Gorbatiikh L, Verpoest I, et al. (2019) Voids in fiber-reinforced polymer composites: A review on their formation, characteristics, and effects on mechanical performance. *J Compos Mater* 53: 1579–1669. <https://doi.org/10.1177/0021998318772152>
27. Wu MS, Centea T, Nutt SR (2018) Compression molding of reused in-process waste—effects of material and process factors. *Adv Manuf Polym Compos Sci* 4: 1–12. <https://doi.org/10.1080/20550340.2017.1411873>
28. Ekuase OA, Anjum N, Eze VO, et al. (2022) A review on the out-of-autoclave process for composite manufacturing. *J Compos Sci* 6: 172. <https://doi.org/10.3390/jcs6060172>
29. Xie J, Wang S, Cui Z, et al. (2019) Process optimization for compression molding of carbon fiber-reinforced thermosetting polymer. *Materials* 12: 2430. <https://doi.org/10.3390/ma12152430>
30. Ochi S (2015) Flexural properties of long bamboo fiber/PLA composites. *Open J Compos Mater* 5: 70–78. <http://dx.doi.org/10.4236/ojcm.2015.53010>

31. Ochi S (2022) Mechanical properties of bamboo fiber bundle-reinforced bamboo powder composite materials. *Eur J Wood Prod* 80: 263–275. <https://doi.org/10.1007/s00107-021-01757-4>
32. Fouly A, Mohamed A, Ibrahim M, et al. (2021) Effect of low hydroxyapatite loading fraction on the mechanical and tribological characteristics of poly(methyl methacrylate) nanocomposites for dentures. *Polymers* 13: 857. <https://doi.org/10.3390/polym13060857>
33. Suarsana K, Astika IM, Sunu PW (2019) Properties of thermal conductivity, density and hardness of aluminium matrices with reinforcement of SiCw/Al<sub>2</sub>O<sub>3</sub> hybrid after sintering process. *IOP Conf Ser Mater Sci Eng* 539: 012016. <https://dx.doi.org/10.1088/1757-899X/539/1/012016>
34. Sathees Kumar S (2020) Dataset on mechanical properties of natural fiber reinforced polyester composites for engineering applications. *Data Brief* 28: 105054. <https://doi.org/10.1016/j.dib.2019.105054>
35. Kumar PAU, Ramalingaiah R, Suresha B, et al. (2018) Mechanical and tribological behavior of vinyl ester hybrid composites. *Tribol Ind* 40: 283–299. <https://doi.org/10.24874/ti.2018.40.02.12>
36. Garg P, Gupta P, Kumar D, et al. (2016) Structural and mechanical properties of graphene reinforced aluminum matrix composites. *J Mater Environ Sci* 7: 1461–1473. Available from: [https://www.jmaterenvironsci.com/Document/vol7/vol7\\_N5/161-JMES-2166-Garg.pdf](https://www.jmaterenvironsci.com/Document/vol7/vol7_N5/161-JMES-2166-Garg.pdf)
37. Nawangsari P, Jamasri, Rochardjo HSB (2019) Effect of phenolic resin on density, porosity, hardness, thermal stability, and friction performance as a binder in non-asbestos organic brake pad. *IOP Conf Ser Mater Sci Eng* 547: 012012. <https://iopscience.iop.org/article/10.1088/1757-899X/547/1/012012>
38. Chen RS, Muhammad YH, Ahmad S (2021) Physical, mechanical and environmental stress cracking characteristics of epoxy/glass fiber composites: Effect of matrix/fiber modification and fiber loading. *Polym Test* 96: 107088. <https://doi.org/10.1016/j.polymertesting.2021.107088>
39. Yawas DS, Aku SY, Amaren SG (2016) Morphology and properties of periwinkle shell asbestos-free brake pad. *J King Saud Univ Eng Sci* 28: 103–109. <https://doi.org/10.1016/j.jksues.2013.11.002>
40. Pisupati A, Ayadi A, Deléglise-Lagardère M, et al. (2019) Influence of resin curing cycle on the characterization of the tensile properties of flax fibers by impregnated fiber bundle test. *Compos Part A Appl Sci Manuf* 126: 105572. <https://doi.org/10.1016/j.compositesa.2019.105572>
41. Sumesh KR, Kanthavel K (2020) The influence of reinforcement, alkali treatment, compression pressure and temperature in fabrication of sisal/coir/epoxy composites: GRA and ANN prediction. *Polym Bull* 77: 4609–4629. <https://doi.org/10.1007/s00289-019-02988-5>
42. Nasution H, Suherman P, Kelvin K, et al. (2020) Mechanical properties of microcrystalline cellulose from coconut fiber reinforced waste styrofoam composite: the effect of compression molding temperature. *IOP Conf Ser Mater Sci Eng* 1003: 012125. <https://dx.doi.org/10.1088/1757-899X/1003/1/012125>
43. Mvondo RRN, Meukam P, Jeong J, et al. (2017) Influence of water content on the mechanical and chemical properties of tropical wood species. *Results Phys* 7: 2096–2103. <https://doi.org/10.1016/j.rinp.2017.06.025>
44. Konsta-Gdoutos MS, Danoglidis PA, Shah SP (2019) High modulus concrete: Effects of low carbon nanotube and nanofiber additions. *Theor Appl Fract Mec* 103: 102295. <https://doi.org/10.1016/j.tafmec.2019.102295>

45. Ismail AS, Jawaid M, Sultan MTH, et al, (2019) Physical and mechanical properties of woven kenaf/bamboo fiber mat reinforced epoxy hybrid composites. *BioResources* 14: 1390–1404. <http://dx.doi.org/10.15376/biores.14.1.1390-1404>
46. Günay M, Korkmaz ME, Özmen R (2020) An investigation on braking systems used in railway vehicles. *Eng Sci Technol* 23: 421–341. <https://doi.org/10.1016/j.jestch.2020.01.009>
47. Jan QMU, Habib T, Noor S, et al. (2020) Multi response optimization of injection moulding process parameters of polystyrene and polypropylene to minimize surface roughness and shrinkage's using integrated approach of S/N ratio and composite desirability function. *Cogent Eng* 7: 1781424. <http://dx.doi.org/10.1080/23311916.2020.1781424>
48. Rangaswamy H, Harsha HM, Chandrashekarappa MPG, et al. (2021) Experimental investigation and optimization of compression moulding parameters for MWCNT/glass/kevlar/epoxy composites on mechanical and tribological properties. *J Mater Res Technol* 15: 327–341. <https://doi.org/10.1016/j.jmrt.2021.08.037>
49. Chen Z, Wang X, Xue B, et al. (2020) Rice husk-based hierarchical porous carbon for high performance supercapacitors: The structure-performance relationship. *Carbon* 161: 432–444. <https://doi.org/10.1016/j.carbon.2020.01.088>
50. Li MX, Lee D, Lee GH, et al. (2020) Effect of temperature on the mechanical properties and polymerization kinetics of polyamide-6 composites. *Polymers* 12: 1133. <https://doi.org/10.3390/polym12051133>
51. Cionita T, Siregar JP, Shing WL, et al. (2022) The influence of filler loading and alkaline treatment on the mechanical properties of palm kernel cake filler reinforced epoxy composites. *Polymers* 14: 3063. <https://doi.org/10.3390/polym14153063>
52. Jang SH, Li LY (2020) Self-sensing carbon nanotube composites exposed to glass transition temperature. *Materials* 13: 259. <https://doi.org/10.3390%2Fma13020259>
53. Lee LT, Tseng HY, Wu TY (2021) Crystallization behaviors of composites comprising biodegradable polyester and functional nucleation agent. *Crystals* 11: 1260. <https://doi.org/10.3390/cryst11101260>



AIMS Press

© 2023 the Author(s), licensee AIMS Press. This is an open access article distributed under the terms of the Creative Commons Attribution License (<http://creativecommons.org/licenses/by/4.0>)